ChemComm

Photo-Induced Formation of Organic Nanoparticles Possessing Enhanced Affinities for Complexing Nerve Agent Mimics

Journal:	*ChemComm*
Manuscript ID	CC-COM-11-2018-008938.R1
Article Type:	Communication

ChemComm

COMMUNICATION

Photo-Induced Formation of Organic Nanoparticles Possessing Enhanced Affinities for Complexing Nerve Agent Mimics†

Received 00th January 20xx,
Accepted 00th January 20xx

DOI: 10.1039/x0xx00000x

www.rsc.org/

Sarah E. Border,[a] Radoslav Z. Pavlović,[a] Lei Zhiquan,[a] Michael J. Gunther,[a] Han Wang,[b] Honggang Cui,[b] Jovica D. Badjić*[a]

Molecular baskets 1^{6-}–3^{6-}, functionalized with α-amino acids at their rim, undergo photo-induced α-decarboxylations to give amphiphilic 4^{3-}–6^{3-} assembling into nanoparticles. Nanoparticulate 4^{3-}–6^{3-} possess greater affinities for complexing OPs (akin to sarin and cyclosarin) than monomeric 1^{6-}–3^{6-}. With the ability of nanoparticles to function in urine, our study sets the stage for creating novel nanocarriers capable of spatiotemporal sequestration of nerve agents or pesticides in competitive chemical environments.

Organophosphorous compounds (OPs) plague society in the form of toxic chemical warfare agents (CWAs) and pesticides.[1] The organization for the prohibition of chemical weapons recently declared that roughly 96% of chemical warfare agents (CWAs) have been eliminated from the world's stockpiles. Despite this, CWAs continue to pose a serious threat to both military personnel and civilians as exemplified by recent events in Syria (Sarin, 2017), UK (Novichok, 2018) and Malaysia (VX, 2018).[2] In essence, *G*- and *V*-type toxicants are OP compounds which act as potent inhibitors of acetylcholinesterase (AChE).[1a] Upon exposure, acetylcholine accumulates in synaptic clefts resulting in seizures, cardiac arrest and asphyxiation. In a related manner, pesticide poisoning presents an important clinical problem around the globe responsible for an estimated 200,000 deaths per year.[3] Along with a steady effort toward developing counter-measures for neutralizing OPs,[4] there is still a need for (a) more effective prophylactics, (b) proper medical treatment of intoxicated individuals, (c) selective scavenging of OPs in peripheral and particularly central nervous systems and (d) inexpensive and quick detection of OPs in minute quantities.[5] Inventing accessible, stimuli-responsive and effective hosts[6] of OPs is expected[7] to facilitate efforts toward their selective detection and removal.[8] Artificial hosts such as cyclodextrins,[9] calixarenes[10] and metal organic frameworks[11] can both detect and degrade nerve agents. Some naturally found bioscavengers such as butyrylcholinesterase (BChE) and paraoxonase 1 (PON1) are also capable of removing CWAs.[12] These natural and non-natural systems utilize non-covalent interactions for fast and, in same cases, reversible complexation of nerve agents. In this vein, we hereby probed light-triggered conversion of hexa-anionic baskets 1^{6-}–3^{6-} into tri-anionic 4^{3-}–6^{3-} (Figure 1A), having increasingly longer amino acids at their periphery, for complexing and removing nerve agent simulants dimethyl methylphosphonate (DMMP, akin in size and shape to sarin; Figure 1B) and dimethyl phenylphosphonate (DMPP, akin in size and shape to cyclosarin; Figure 1B).[13] Since monomeric 2^{6-} undergoes photo-induced α-decarboxylation to give 5^{3-}, assembling into nanoparticles,[13a] we wondered if 1^{6-} and 3^{6-} would show similar stimuli-responsive characteristics. If so, will the light-produced nanoparticulate 4^{3-}–6^{3-} possess different affinities

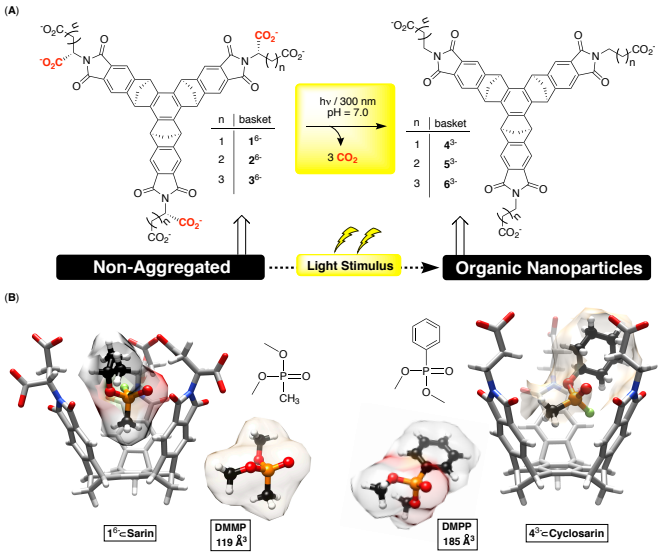

Figure 1 . (A) Chemical structures of baskets 1^{6-}–3^{6-} and products of their photo-induced α-decarboxylation 4^{3-}–6^{3-}. (B) Energy-minimized (Spartan, MMFF) structures of DMMP (left) akin to sarin (132 Å^3) in size and shape and DMPP (right) akin to cyclosarin (174 Å^3). Energy-minimized (Spartan, MMFF) structures of basket 1^{6-} holding sarin and 4^{3-} with cyclosarin.

[a] Department of Chemistry & Biochemistry, The Ohio State University 100 West 18th Avenue, 43210 Columbus, Ohio USA. E-mail: badjic.1@osu.edu
[b] Department of Chemical and Biomolecular Engineering, The Johns Hopkins University Maryland Hall 221, 3400 North Charles Street, 21218 Baltimore, Maryland USA

† Electronic Supplementary Information (ESI) available: [Experimental details, additional spectra and computations]. See DOI: 10.1039/x0xx00000x

than non-aggregated $\mathbf{1}^{6-}$–$\mathbf{3}^{6-}$ for binding OPs? As nanocarriers[14] of CWAs ought to be functional in biological fluids,[15] we aimed to examine the capacity of organic nanoparticles composed of molecular baskets to bind OPs from synthetic urine for their potential application as nanostructured sequestering agents in biological systems.

Molecular baskets $\mathbf{1}^{6-}$ and $\mathbf{3}^{6-}$ (Figure 1A) were prepared using established synthetic procedures[13a] and characterized with one/two dimensional NMR spectroscopic methods (Figure S1-S7). First, we examined the aggregation and photochemical characteristics of $\mathbf{1}^{6-}$ conjugated to three shorter (*R*/*S*)–aspartic acids and $\mathbf{3}^{6-}$ with longer

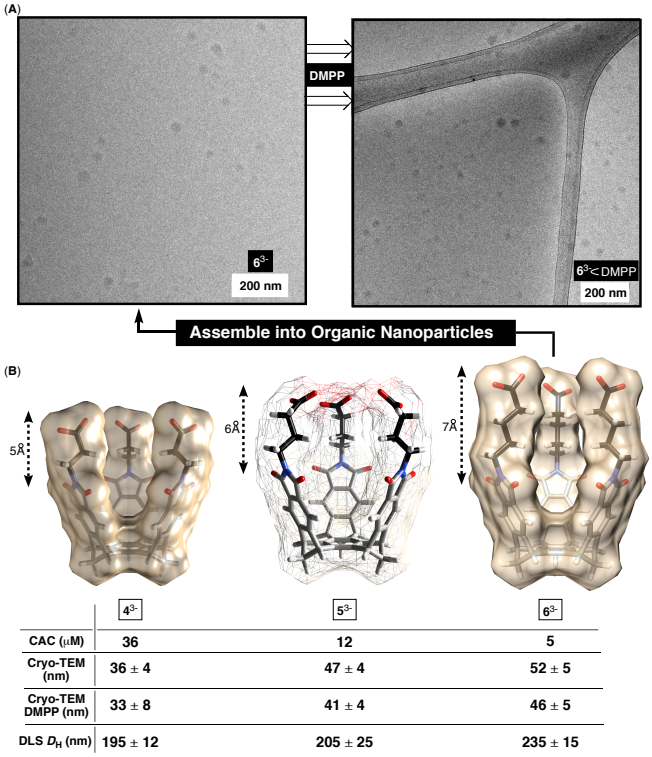

	$\mathbf{4}^{3-}$	$\mathbf{5}^{3-}$	$\mathbf{6}^{3-}$
CAC (μM)	36	12	5
Cryo-TEM (nm)	36 ± 4	47 ± 4	52 ± 5
Cryo-TEM DMPP (nm)	33 ± 8	41 ± 4	46 ± 5
DLS D_H (nm)	195 ± 12	205 ± 25	235 ± 15

Figure 2 (A) Cryo-TEM images of $\mathbf{6}^{3-}$ (1.0 mM in 30 mM phosphate buffer at pH = 7.0) without and with ten molar equivalents of DMPP. (B) van der Waals surfaces of $\mathbf{4}^{3-}$, $\mathbf{5}^{3-}$ and $\mathbf{6}^{3-}$ (Chimera), along with CAC and size (diameter) of nanoparticles.

(*S*)–2-aminoadipic acids. ^{1}H NMR spectra of 0.1 mM baskets $\mathbf{1}^{6-}$ and $\mathbf{3}^{6-}$, each dissolved in 30 mM phosphate buffer at pH = 7.0, showed a set of narrow resonances (Figure S15A). In particular, a sixteen-fold dilution of $\mathbf{1}^{6-}$ (1.1–0.07 mM, Figure S16) had no effect on the line width and the overall splitting pattern of its ^{1}H NMR signals, thereby suggesting the monomeric state of the host within this concentration range. Indeed, the apparent hydrodynamic radius r_H = 8.4 Å (PFG NMR, Figure S17) of 0.5 mM solution of $\mathbf{1}^{6-}$ (D_{app} = 2.8 · 10^{-10} m^2/s) is comparable to its computationally estimated radius of circa 10 Å (MM/MC, OPLS-3; Figures S44-S45). From variable concentration ^{1}H NMR spectra of $\mathbf{3}^{6-}$ (Figure S18), however, we noted the "sharpening" of its resonances occurring between 0.5 and 1.0 mM solutions. PFG NMR measurements of the apparent diffusion coefficient (D_{app} = 2.9 · 10^{-10} m^2/s) of diluted $\mathbf{3}^{6-}$ (0.3 mM, Figure S19) produced r_H = 8.5 (Figures S44-S45). Dynamic light scattering (DLS) measurements of more concentrated 1.0 mM solution of $\mathbf{3}^{6-}$, however, showed the presence of particles 212 ± 7 nm in diameter (Figure S20). To sum up, basket $\mathbf{3}^{6-}$ appears to transition from monomeric to assembled states within 0.5 to 1.0 mM range of concentrations. For our study, we used aqueous $\mathbf{1}^{6-}$–$\mathbf{3}^{6-}$ at concentrations whereby these hosts are predominantly monomeric.

Table 1. Thermodynamic stabilities (K_a, M^{-1}) of complexes of baskets $\mathbf{1}^{6-}$–$\mathbf{3}^{6-}$ and $\mathbf{4}^{3-}$–$\mathbf{6}^{3-}$ with OPs in 30 mM phosphate buffer at pH = 7.0 ± 0.1 were determined with ^{1}H NMR Spectroscopy (298 K, Figures S27-38). Each value of K_a is reported as an arithmetic mean of two measurements with standard deviation as the margin of error.

K_a (M^{-1})	$\mathbf{1}^{6-}$ → $\mathbf{4}^{3-}$		$\mathbf{2}^{6-}$ → $\mathbf{5}^{3-}$		$\mathbf{3}^{6-}$ → $\mathbf{6}^{3-}$	
DMMP	19 ± 7	447 ± 54	29 ± 1	311 ± 99	59 ± 4	280 ± 47
DMPP	151 ± 60	8891 ± 192	213 ± 7	3943 ± 407	717 ± 7	2547 ± 69

The irradiation (300 nm, Rayonet) of 0.1 mM solutions of $\mathbf{1}^{6-}$ and $\mathbf{3}^{6-}$ was monitored with ^{1}H NMR spectroscopy to show a steady decrease in the intensity of baskets' resonances (Figures S21–S22). It took approximately 20-40 minutes for ^{1}H NMR signals to, in each case, cease changing albeit amounting to ill-defined ^{1}H NMR spectra (Figure S15). We suspected[13a] that the observed spectroscopic changes resulted from the aggregation of $\mathbf{4}^{3-}$ and $\mathbf{6}^{3-}$ yet photochemical reactions could also be taking another turn.[16] After stopping the irradiation, each sample was acidified and the collected precipitate subjected to lyophilization. The remaining solid was dissolved in DMSO-d_6 to show a set of sharp ^{1}H NMR signals corresponding to $\mathbf{4}^{3-}$ and $\mathbf{6}^{3-}$ (Figures S8-S15).[13a] As in the case of basket $\mathbf{2}^{3-}$,[13a] the irradiation of monomeric $\mathbf{1}^{6-}$ and $\mathbf{3}^{6-}$ thus leads to the exclusive removal of three α-carboxylates to give $\mathbf{4}^{3-}$ and $\mathbf{6}^{3-}$ aggregating in water. Cryo-TEM and conventional TEM micrographs of aqueous $\mathbf{4}^{3-}$ and $\mathbf{6}^{3-}$ (Figure 2A; Figures S39-S43) revealed the formation of nanoparticles with a distribution of diameters 36 ± 4 and 52 ± 5 nm (Figure 2B). In addition, the results of DLS measurements (Figure 2B; Figures S23-S24) suggested the existence of particles with averaged hydrodynamic diameter D_H of 195 ± 12 and 235 ± 15 nm for $\mathbf{4}^{3-}$ and $\mathbf{6}^{3-}$, respectively. Critical aggregation concentrations (CAC) of $\mathbf{4}^{3-}$, $\mathbf{5}^{3-}$ and $\mathbf{6}^{3-}$ were found to be 36, 12 and 5 μM (Figure 3B; see also Figures S25–S26). First, both cryo-TEM and DLS measurements showed a small but steady increase in the size of nanoparticulate $\mathbf{4}^{3-}$, $\mathbf{5}^{3-}$ and $\mathbf{6}^{3-}$ (Figure 2B).[13a] As increasingly longer amino acids contribute to the formation of larger nanoparticles, we deduce that baskets ought to be assembling in a similar fashion. Second, increasingly longer amino acid chains at the rim of $\mathbf{4}^{3-}$, $\mathbf{5}^{3-}$ and $\mathbf{6}^{3-}$ give more stable aggregates with lower CAC (Figure 2B). Perhaps, van der Waals contacts between progressively longer alkyl groups (Figure 2B) along with their more favorable desolvation contribute to greater stability of the nanomaterial along the series.[17]

Will the photo-induced formation of nanoparticles have an effect on the complexation of OPs (Figure 3)? With the assistance of ^{1}H NMR spectroscopy, we probed the binding of DMMP and DMPP to $\mathbf{1}^{6-}$–$\mathbf{3}^{6-}$ (Table 1). Nonlinear least-square analyses of biding isotherms (Figure S27-S32), along with distribution of residuals,[18] suggested the formation of binary complexes with K_a<717 M^{-1} (Figure 3A). In the same manner, NMR data for the complexation of DMMP/DMPP to nanoparticulate $\mathbf{4}^{3-}$–$\mathbf{6}^{3-}$ (Figures S33-S38) was in line with the predominant formation of more stable binary complexes (K_a<10000 M^{-1}, Figure 3B). Last, cryo-TEM micrographs provided evidence that binary $\mathbf{4}^{3-}$–$\mathbf{6}^{3-}$⊂DMPP assemble into nanoparticles (Figure 2A; Figures S39-S41).

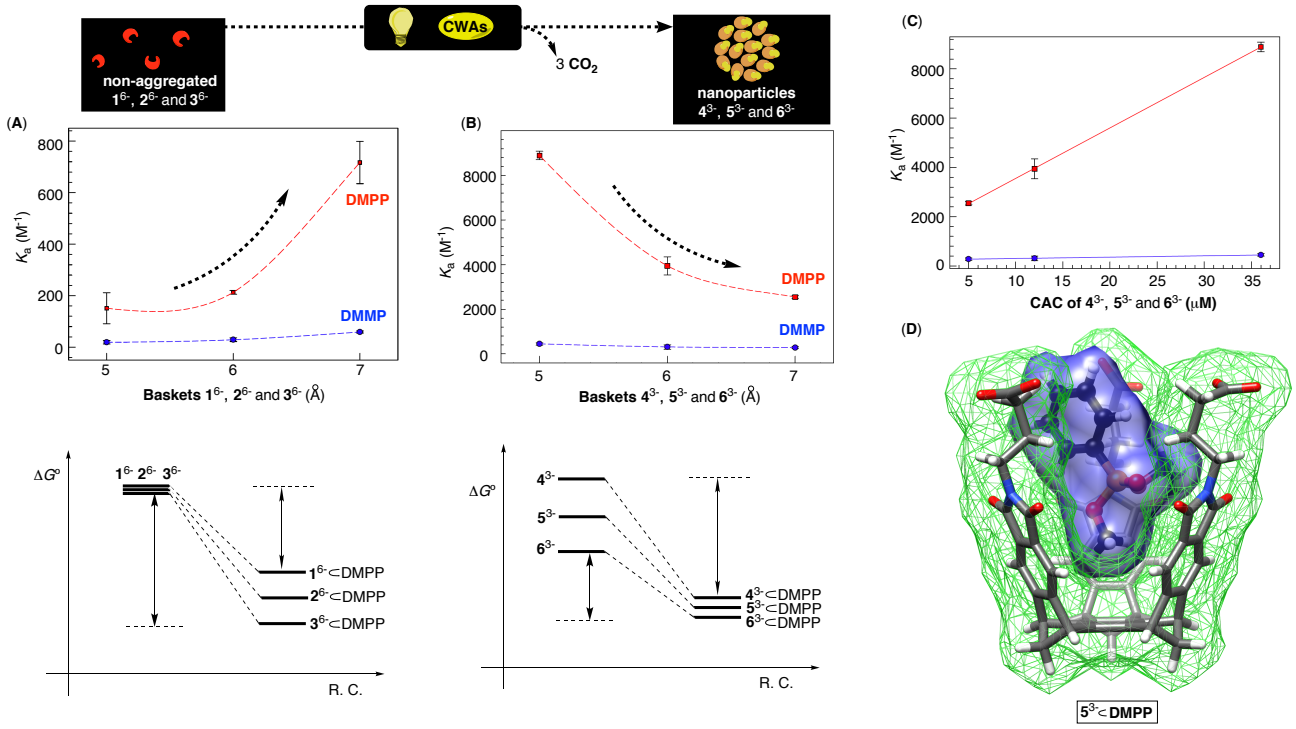

Figure 3 (A) Binding affinity K_a (M^{-1}) of $\mathbf{1}^{6-}$–$\mathbf{3}^{6-}$ toward DMMP (blue) and DMPP (red) as a function of the length of their peripheral chains. Reaction coordinate diagram (RCD) depicting the complexation of OPs. (B) Binding affinity K_a (M^{-1}) of $\mathbf{4}^{3-}$–$\mathbf{6}^{3-}$ toward DMMP (blue) and DMPP (red) as a function of the length of their peripheral chains. RCD depicting the complexation of OPs. (C) Binding affinity K_a (M^{-1}) of $\mathbf{4}^{3-}$–$\mathbf{6}^{3-}$ toward DMMP (blue) and DMPP (red) as a function of their CAC (μM). (D) Energy-minimized structure of $\mathbf{5}^{3-}$⊂DMPP showing its van der Waals surfaces (Spartan, MMFF).

From the dependence of binding affinities K_a as a function of the length of amino acids in **1**–**6** (Figure 3A/B), we deduced about the nature of the recognition. First, all six hosts possess a greater affinity for DMPP (185 Å^3) than DMMP (119 Å^3). With the assistance of 3V software,[19] we estimated the inner volume of $\mathbf{4}^{3-}$ (230Å^3), $\mathbf{5}^{3-}$ (240 Å^3) and $\mathbf{6}^{3-}$ (257 Å^3). If fully inserted into these hosts, DMPP would occupy 72–80% while DMMP 46–52% of the interior space of $\mathbf{4}^{3-}$–$\mathbf{6}^{3-}$.[20] With the examined OPs protruding their groups through side apertures (Figure 3D), the occupancy factor becomes a less reliable indicator of the stability.[20] Nonetheless, larger DMPP forms more contacts with baskets than DMMP to elicit more extensive desolvation to, in this way, more effectively drive the association.[21] Second, nanoparticulate $\mathbf{4}^{3-}$–$\mathbf{6}^{3-}$ form more stable complexes with OPs than monomeric $\mathbf{1}^{6-}$–$\mathbf{3}^{6-}$ (Figure 3A/B). On the basis of an earlier study,[13g] α-carboxylates at the rim of $\mathbf{1}^{6-}$–$\mathbf{3}^{6-}$ are likely to obstruct the docking of juxtaposed OPs via unfavorable contacts. Such steric strain is, however, absent in $\mathbf{4}^{3-}$–$\mathbf{6}^{3-}$ enabling stronger host-guest contacts. In addition to the enthalpic effects, entropy may also play a role: as a result of packing, $\mathbf{4}^{3-}$–$\mathbf{6}^{3-}$ possess lower degrees of freedom. This, in turn, is expected to improve the preorganization[21] and augment the stability of host-guest complexes. Third, the affinity of monomeric $\mathbf{1}^{6-}$–$\mathbf{3}^{6-}$ for complexing OPs (Figure 3A) increases with longer amino acids at their periphery implying that deeper and more hydrophobic pockets are more accommodating for OPs. As already discussed, increasing the contact area between two nonpolar molecules in a polar solvent should benefit the system's free energy ΔG° (see RCD in Figure 3A) from additional non- covalent interactions ($\Delta H^{\circ}<0$) and/or greater desolvation ($\Delta S^{\circ}>0$).[17] Fourth, deepening tri-anionic $\mathbf{4}^{3-}$–$\mathbf{6}^{3-}$ (Figure 3B) was found to have an adverse effect on the formation of the corresponding binary complexes. To explain the dichotomy with respect to $\mathbf{1}^{6-}$–$\mathbf{3}^{6-}$, we noted that plotting K_a for the formation of $\mathbf{4}^{3-}$

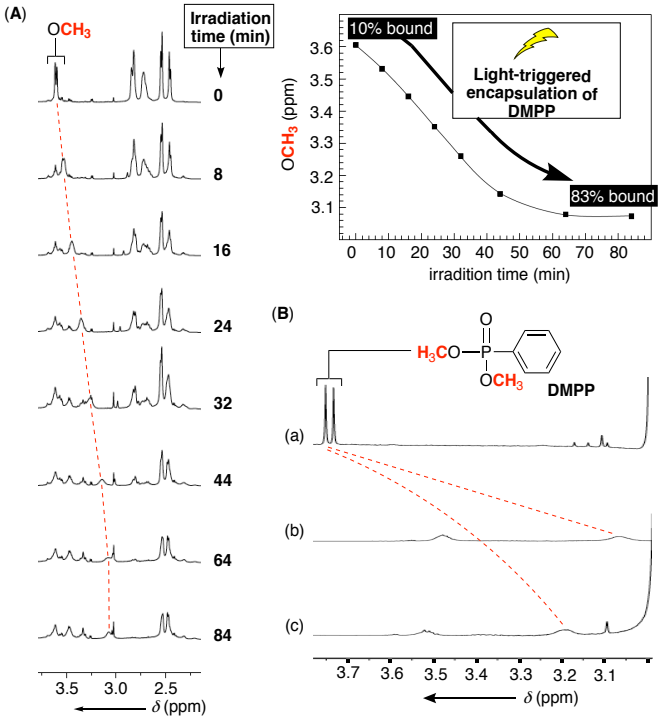

Figure 4. (A) ^{1}H NMR spectra (700 MHz, 298.0 K) of 0.8 mM solution of $\mathbf{1}^{6-}$ containing 0.4 molar equivalents of DMPP (30.0 mM phosphate buffer at pH = 7.0 ± 0.1) and after irradiation at 300 nm. Percentages based on experimentally determined K_a's of $\mathbf{1}^{6-}$ and $\mathbf{4}^{3-}$ (Right) A change in the magnetic shielding of OCH_3 resonance from DMPP with the irradiation time. (B) Partial ^{1}H NMR spectra (600 MHz, 298 K) of (a) 0.2 mM DMPP in Surine, (b) 0.3 mM $\mathbf{4}^{3-}$ in 30 mM phosphate buffer (pH = 7.0) containing 0.2 mM DMPP and (c) 0.3 mM $\mathbf{4}^{3-}$ in Surine, containing 0.2 mM DMPP.

–$\mathbf{6}^{3-}$⊂DMMP (blue, Figure 3C) and $\mathbf{4}^{3-}$–$\mathbf{6}^{3-}$⊂DMPP (red, Figure 4C) as a function of CAC showed a linear dependence with the most stable and nanoparticulate $\mathbf{6}^{3-}$ having the smallest affinity toward OPs. Seemingly, thermodynamic stability of the assembled $\mathbf{4}^{3-}$–$\mathbf{6}^{3-}$ has an effect on nanoparticle-to-nanoparticle transition, constituting the encapsulation. That is to say, if the stability difference between aggregated $\mathbf{4}^{3-}$,$\mathbf{5}^{3-}$ and $\mathbf{6}^{3-}$ (RCD in Figure 3B) is large enough it could have an effect on the encapsulation driving force (ΔGº): for accommodating OPs, more stable nanoparticles $\mathbf{6}^{3-}$ are more difficult to reorganize than less stable $\mathbf{4}^{3-}$; on the other hand, monomeric $\mathbf{1}^{6-}$–$\mathbf{3}^{6}$ did not need to "invest reorganizational energy" for trapping OPs, with the observed affinities tracking the intrinsic stability of the complexed species (RCD in Figure 3A). The mechanism by which the recognition takes place remains unknown yet a small reduction in the size of nanoparticles after the complexation (Figure 2B) is in line with their dynamic nature. At last, UV irradiation of an aqueous solution of $\mathbf{1}^{6-}$ and DMPP led to photo-induced removal of basket's α-carboxylates and the formation of $\mathbf{4}^{3-}$ reducing the concentration of free DMPP from 90% to 17% (Figure 4A; Figure S44). Moreover, when basket $\mathbf{4}^{3-}$ was added to synthetic urine (Surine™) containing DMPP, the extent of the magnetic shielding of its proton nuclei (Figure 4B; Figure S45) was comparable to the control experiment in phosphate buffer.

In conclusion, photo-responsive[22] baskets can be prompted with light to undergo α-decarboxylation and give amphiphilic hosts. The hosts assemble into nanoparticles able to trap OPs, akin is size and shape to *G*-type nerve agents. Importantly, the affinity of nanoparticulate material for complexing OPs is greater than of non-aggregated baskets. As the recognition of OPs with these nanostructured materials takes place in urine, our findings should, in particular, serve as a rudimentary guide for developing light-responsive nanocarriers[23] capable of selective, spatial and temporal sequestration of nerve agents or pesticides in competitive and complex biological environments.

Conflicts of interest

There are no conflicts to declare.

Acknowledgements

This work was financially supported with funds obtained from the National Science Foundation under CHE-1606404. We thank CCIC facility at the OSU for providing support in completing NMR spectroscopic measurements.

References

1. (a) K. Kim, O. G. Tsay, D. A. Atwood and D. G. Churchill, *Chem. Rev.*, 2011, **111**, 5345; (b) S. Costanzi, J.-H. Machado and M. Mitchell, *ACS Chem. Neurosci.*, 2018, **9**, 873.
2. R. Chai Peter, R. Chai Peter, W. Boyer Edward, D. Hayes Bryan and B. Erickson Timothy, *Toxicol Commun*, 2018, **2**, 45.
3. M. Eddleston, N. A. Buckley, P. Eyer and A. H. Dawson, *Lancet*, 2008, **371**, 597.
4. P. Masson, *Phosphorus, Sulfur Silicon Relat. Elem.*, 2016, **191**, 1433.
5. (a) E. Dolgin, *Nat Med*, 2013, **19**, 1194; (b) F. M. Raushel, *Nature*, 2011, **469**, 310; (c) L. Chen, D. Wu and J. Yoon, *ACS Sens.*, 2018, **3**, 27; (d) G. Mercey, T. Verdelet, J. Renou, M. Kliachyna, R. Baati, F. Nachon, L. Jean and P.-Y. Renard, *Acc. Chem. Res.*, 2012, **45**, 756; (e) R. R. Butala, W. R. Creasy, R. A. Fry, M. L. McKee and D. A. Atwood, *Chem. Commun.*, 2015, **51**, 9269; (f) V. Kumar, G. Raviraju, H. Rana, V. K. Rao and A. K. Gupta, *Chem. Commun.*, 2017, **53**, 12954.
6. (a) S. E. Border, R. Z. Pavlovic, L. Zhiquan and J. D. Badjic, *J. Am. Chem. Soc.*, 2017, **139**, 18496; (b) K. Uzarevic, T. C. Wang, S.-Y. Moon, A. M. Fidelli, J. T. Hupp, O. K. Farha and T. Friscic, *Chem. Commun.*, 2016, **52**, 2133.
7. M. R. Sambrook and S. Notman, *Chem. Soc. Rev.*, 2013, **42**, 9251.
8. (a) Y.-C. Yang, *Acc. Chem. Res.*, 1999, **32**, 109; (b) V. V. Singh, K. Kaufmann, B. Esteban-Fernandez de Avila, M. Uygun and J. Wang, *Chem. Commun.*, 2016, **52**, 3360.
9. S. Letort, S. Balieu, W. Erb, G. Gouhier and F. Estour, *Beilstein J. Org. Chem.*, 2016, **12**, 204.
10. C. Schneider, A. Bierwisch, M. Koller, F. Worek and S. Kubik, *Angew. Chem., Int. Ed.*, 2016, **55**, 12668.
11. M. J. Katz, J. E. Mondloch, R. K. Totten, J. K. Park, S. B. T. Nguyen, O. K. Farha and J. T. Hupp, *Angew. Chem., Int. Ed.*, 2014, **53**, 497.
12. F. Nachon, X. Brazzolotto, M. Trovaslet and P. Masson, *Chem. Biol. Interact.*, 2013, **206**, 536.
13. (a) S. E. Border, R. Z. Pavlovic, L. Zhiquan, M. J. Gunther, H. Wang, H. Cui and J. D. Badjic, *Chem. Eur. J.*, 2018, DOI: 10.1002/chem.201803693, Ahead of Print; (b) S. Chen, S. M. Polen, L. Wang, M. Yamasaki, C. M. Hadad and J. D. Badjic, *J. Am. Chem. Soc.*, 2016, **138**, 11312; (c) S. Chen, Y. Ruan, J. D. Brown, J. Gallucci, V. Maslak, C. M. Hadad and J. D. Badjic, *J. Am. Chem. Soc.*, 2013, **135**, 14964; (d) S. Chen, Y. Ruan, J. D. Brown, C. M. Hadad and J. D. Badjic, *J. Am. Chem. Soc.*, 2014, **136**, 17337; (e) S. Chen, L. Wang, S. M. Polen and J. D. Badjic, *Chem. Mater.*, 2016, **28**, 8128; (f) Y. Ruan, S. Chen, J. D. Brown, C. M. Hadad and J. D. Badjic, *Org. Lett.*, 2015, **17**, 852; (g) Y. Ruan, E. Dalkilic, P. W. Peterson, A. Pandit, A. Dastan, J. D. Brown, S. M. Polen, C. M. Hadad and J. D. Badjic, *Chem. Eur. J.*, 2014, **20**, 4251; (h) L. Wang, T. Neal, S. Chen and J. D. Badjic, *Chem. Eur. J.*, 2017, **23**, 8829.
14. J.-C. Leroux, *Nat. Nanotechnol.*, 2007, **2**, 679.
15. Z. Pang, C.-M. J. Hu, R. H. Fang, B. T. Luk, W. Gao, F. Wang, E. Chuluun, P. Angsantikul, S. Thamphiwatana, W. Lu, X. Jiang and L. Zhang, *ACS Nano*, 2015, **9**, 6450.
16. A. G. Griesbeck, W. Kramer and M. Oelgemoller, *Synlett*, 1999, DOI: 10.1055/s-1999-3159, 1169.
17. B. C. Gibb, *Chemosensors*, 2011, DOI: 10.1002/9781118019580.ch1, 3.
18. D. Brynn Hibbert and P. Thordarson, *Chem. Commun.*, 2016, **52**, 12792.
19. Y. Ruan, B.-Y. Wang, J. M. Erb, S. Chen, C. M. Hadad and J. D. Badjic, *Org. Biomol. Chem.*, 2013, **11**, 7667.
20. S. Mecozzi and J. Rebek, Jr., *Chem. Eur. J.*, 1998, **4**, 1016.
21. J. B. Wittenberg and L. Isaacs, *Supramol. Chem. Mol. Nanomater.*, 2012, **1**, 25.
22. D.-H. Qu, Q.-C. Wang, Q.-W. Zhang, X. Ma and H. Tian, *Chem. Rev.*, 2015, **115**, 7543.
23. N. Bertrand, C. Bouvet, P. Moreau and J.-C. Leroux, *ACS Nano*, 2010, **4**, 7552.

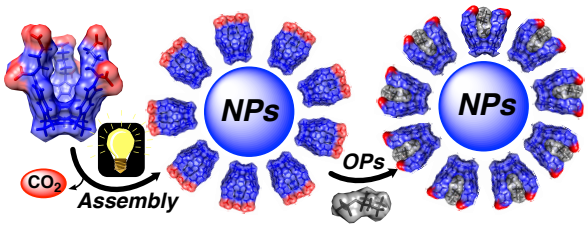

Organic nanoparticles, composed of molecular baskets, could act as nanocarriers for selective "mopping" of toxic CWAs or pesticides, after being assembled by a light stimulus.